Journal of Hazardous Materials 189 (2011) 502–508

Contents lists available at ScienceDirect

Journal of Hazardous Materials

journal homepage: www.elsevier.com/locate/jhazmat

Investigation of cation (Sn^{2+}) and anion (N^{3-}) substitution in favor of visible light photocatalytic activity in the layered perovskite $K_2La_2Ti_3O_{10}$

Vinod Kumar[a], Govind[b], S. Uma[a,*]

[a] Materials Chemistry Group, Department of Chemistry, University of Delhi, Delhi 110007, India
[b] Physics of Energy Harvesting, National Physical Laboratory (CSIR), Dr. K. S. Krishnan Marg, New Delhi 110 012, India

ARTICLE INFO

Article history:
Received 8 November 2010
Received in revised form 11 February 2011
Accepted 19 February 2011
Available online 26 February 2011

Keywords:
Layered perovskite
Tin doping
Nitrogen incorporation
Visible absorption
Photocatalyst
Rhodamine B

ABSTRACT

Noticeable lowering of the energy gaps have been achieved for the layered perovskite $K_2La_2Ti_3O_{10}$ as a result of the attempts made to incorporate Sn^{2+} and N^{3-} ions. Incorporation of Sn^{2+} ions was carried out by the ion-exchange reaction of $K_2La_2Ti_3O_{10}$ with aqueous tin(II) chloride solution. Nitrogen incorporation was attempted by the solid state reaction of the parent oxide with urea around 400 °C in air. The resultant oxides have been characterized by power X-ray diffraction, UV–visible diffuse reflectance spectroscopy, and Fourier transform infrared spectroscopy. Room temperature ion-exchange was sufficient to introduce Sn^{2+} ions with the resulting product of composition $(Sn_{0.45}K_{0.2}H_{0.9})La_2Ti_3O_{10}\cdot H_2O$. Visible light absorption was observed with the absorption edge red shift of ~100 nm from that of the parent $K_2La_2Ti_3O_{10}$. The lowering of the band gap was as expected by the contribution of Sn 5s orbitals to the O 2p orbitals in the formation of the valence band. Nitridation using urea resulted not only in nitrogen doping but with the additional sensitization by the presence of carbon nitride (CN) polymers, which again resulted in visible light absorption. The product oxides obtained as a result of cation and anion intended substitutional studies have been found to be useful for the visible light photocatalytic decomposition of organic dyes such as rhodamine B.

1. Introduction

The development of new semiconductor based photocatalytic materials is a very challenging task, for it involves different deciding factors such as the band gap, carrier transport, catalytic activity, surface related absorption properties and chemical stability [1]. Presently, TiO_2 with a band gap of 3.2 eV (387.5 nm) has been the most accepted and widely used photocatalyst for the mineralization of various harmful organic compounds and for the successful splitting of water to produce hydrogen and oxygen [2–4]. The searches for alternate photocatalysts are being carried out to develop materials that are capable of using visible light, which constitutes a larger portion of the solar light. One approach has been to modify the band gap of TiO_2 by metal (e.g. Cr, Fe, Mn, V, Mo, Co, Ni) ion doping. In spite of the successful reports of visible light activity, specially for Cr^{3+} and Fe^{3+} doped TiO_2, faster recombination of electrons and holes occur due to the formation of defects by cation doping [3–6]. Recently, incorporation of non metal dopants such as C, N, F, S, and P in TiO_2 has attracted the attention of the researchers [6–10] and in particular nitrogen doping has been extensively investigated [11–13]. Narrowing of the band gap leading to visible light absorption and photocatalytic activity has been attributed to the overlap of N 2p and O 2p orbitals in the formation of the valance band.

Another important route to discover photocatalysts has been to identify new materials with appropriate band gaps. Many mixed metal oxides with early transition metal ions having d^0 configuration (Ti^{4+}, Nb^{5+}, Ta^{5+}) have been explored. Specifically, several of the layered perovskites such as $K_2La_2Ti_3O_{10}$, $RbPb_2Nb_3O_{10}$, $KLaNb_2O_7$, have been identified as photocatalysts in the presence of co-catalysts (Pt, NiO, etc.) for the evolution of H_2 from water under UV light radiation [14]. These layered oxides are attractive photocatalytic materials for the following reasons: (i) their structures consist of two dimensional perovskite slabs interleaved with cations and this structural type is expected to increase the lifetime of the photogenerated electrons and holes, and thereby increasing the efficiency of the materials [15]; (ii) the perovskite slabs are normally made up of metals such as Ti, Nb, or Ta, that have been preferred as photocatalysts under UV irradiation [14]; (iii) numerous low temperature synthetic possibilities exist [16] to study the influence of cationic and/or anionic substitutions by the appropriate tuning of the band gaps. For the aforementioned reasons, we were interested to investigate the layered perovskite oxide, $K_2La_2Ti_3O_{10}$ as part of our ongoing efforts to identify visible light active photocatalysts for the decomposition of aqueous dye solutions [17–19].

* Corresponding author. Fax: +91 11 27666605.
E-mail address: suma@chemistry.du.ac.in (S. Uma).

0304-3894/$ – see front matter © 2011 Elsevier B.V. All rights reserved.
doi:10.1016/j.jhazmat.2011.02.064

Our objective has been to study the influence of cationic (Sn^{2+} for K^+) and anionic (N^{3-} for O^{2-}) substitutions, in order to verify the changes in the band gaps along with the photocatalytic activities. Incorporation of Sn^{2+} with a $5s^2$ configuration has resulted in lowering of the band gaps similar to the effect of nitrogen incorporation leading to visible light absorption and subsequent photocatalytic activities. Particularly, experiments supported by theoretical calculations in the case of oxides such as SnM_2O_6 and SnM_2O_7 (M = Nb, Ta) have indicated the formation of valence bands by the mixing of O 2p and Sn 5s orbitals. Specifically, $SnNb_2O_6$, photocatalytically evolved H_2 and O_2 from water under visible light [20]. $SnWO_4$ exhibited good photocatalytic activity for the degradation of rhodamine B dye solution under visible light [21]. Sn^{2+} incorporation by simple ion-exchange reactions has been known in the synthesis of various photocatalysts such as $Sn^{2+}/K_4Nb_6O_{17}$, $Sn^{2+}/KTiNbO_5$ which produce H_2 from an aqueous methanolic solution under visible light irradiation [22]. We recently reported the simple ion-exchange synthesis of novel Sn^{2+} containing pyrochlore oxides such as $Sn_{0.92}Sb_2O_6{\cdot}2.0H_2O$, $K_{0.59}Sn_{0.20}SbWO_6{\cdot}1.0H_2O$ and $K_{0.58}Sn_{0.29}TaWO_6{\cdot}1.0H_2O$ and investigated their photophysical and photocatalytic properties [18]. To our knowledge, $K_2La_2Ti_3O_{10}$ has not been exchanged with Sn^{2+} ions, and we wanted to examine if potassium ions can be replaced by Sn^{2+} ions by simple ion-exchange reactions and if so, interested in determining the effect of Sn^{2+} ions substitution on the visible light absorption and the photocatalytic activities. In the present study, we synthesized Sn^{2+} incorporated $K_2La_2Ti_3O_{10}$ by the room temperature ion-exchange reaction of $K_2La_2Ti_3O_{10}$ with an aqueous solution of tin (II) chloride solutions. Band gap was reduced in the resultant Sn^{2+} exchanged $K_2La_2Ti_3O_{10}$ product and was found to decompose aqueous rhodamine B (Rh B) solution under visible light.

Regarding the anionic (N^{3-}) substitution in $K_2La_2Ti_3O_{10}$, it is significant to mention that many mixed metal oxides have also been systematically researched for nitrogen doping, as in the case of TiO_2. Band gap narrowing due to the upward lifting of the valence band by N 2p contribution and visible light photocatalytic activities have been observed in the case of layered niobate, HNb_3O_8 [23], layered titanate, $Cs_{0.68}Ti_{1.83}O_4$ [24], and the three dimensional perovskite, $SrTiO_3$ [25]. Nitrogen incorporated $K_2La_2Ti_3O_{10}$ was also synthesized using urea with a view to compare the band gap narrowing between the cation (Sn^{2+}) substituted and the anion (N^{3-}) substituted products. However, we found that by heating the oxide $K_2La_2Ti_3O_{10}$ with urea in air around 400 °C resulted not only in nitrogen doping but with the additional sensitization by the presence of carbon nitride (CN) polymers. Polymeric graphitic carbon nitrides, g-C_3N_4, and metal (Fe, Zn) containing g-C_3N_4 have proven to be efficient visible light photocatalysts [26,27]. Nitrogen doping coupled with the incorporation of CN polymers in oxides were known, specially when urea was used as the source of nitrogen. Furthermore, the carbon and nitrogen based condensation products of melamine obtained by the thermolysis of compounds such as urea act as sensitizers resulting in increased UV and/or visible light photocatalytic activities in the case of TiO_2 [28], $NaNbO_3$ [29] and $H_2Ta_2O_7$ [30]. Currently, in $K_2La_2Ti_3O_{10}$, we observed that nitrogen doping along with the introduction of CN polymers contributed to the lowering of the band gap leading to visible light photocatalytic degradation of aqueous Rh B solution.

2. Experimental

The parent $K_2La_2Ti_3O_{10}$ was prepared by mixing and heating stoichiometric amounts of K_2CO_3 (Ranbaxy), pre dried La_2O_3 (99.9%, Aldrich) and TiO_2 (99.8%, Aldrich), initially at 900 °C for 12 h, then reground and calcined at 1000 °C for 12 h. The powder X-ray diffraction confirmed that the white product was essentially $K_2La_2Ti_3O_{10}$.

2.1. Ion-exchange synthesis of $Sn^{2+}/K_2La_2Ti_3O_{10}$

After the structural verification by powder X-ray diffraction, the parent $K_2La_2Ti_3O_{10}$ was ion-exchanged with a solution of $SnCl_2{\cdot}2.0H_2O$ (99.99%, Aldrich) in acidic medium. Typically, 1 g of the powder was sonicated with 100 ml of 0.1 M tin (II) chloride solution in hydrochloric acid for 2 h and the white color of the powder changed instantaneously to yellowish green. The products after ion-exchange were washed with water and dried at room temperature.

2.2. Synthesis of nitrogen incorporated $K_2La_2Ti_3O_{10}$

Typically, 1 g of the parent layered perovskite was mixed with 4 g of urea (99.5%, Spectrochem) and then heated in a covered crucible at 400 °C in air for 3 h. For comparison, nitrogen incorporation in $K_2La_2Ti_3O_{10}$ was tried at 400 °C for 6 h by heating under ammonia vapor using nitrogen as the purge gas.

2.3. Characterization

The powder X-ray diffraction patterns were recorded using Rigaku Miniflex diffractometer employing Cu Kα radiation. QUANTA 200 FEG (FEI Netherlands) Scanning Electron Microscope and Zeiss EVO-40 Scanning Electron Microscope with EDAX attachment were used to obtain the cation stoichiometry. Morphology of the samples were also recorded using Philips Technai G^2 TEM with 300 kV accelerating voltage. UV–visible diffuse reflectance data was collected over the spectral range 200–1000 nm using Perkin Elmer Lambda 35 scanning double beam spectrometer equipped with a 50 mm integrating sphere. $BaSO_4$ was used as a reference. The data were transformed into absorbance with the Kubelka–Munk function. Fourier Transform Infra Red spectroscopy was taken using a Perkin Elmer 2000 spectrometer. The chemical nature of N in the urea treated $K_2La_2Ti_3O_{10}$ has been studied using X-ray photoelectron spectroscopy (XPS) using Perkin Elmer series XPS using an Al Kα X-ray line (*hv*-1486.6 eV) for photoelectron excitation.

2.4. Photocatalytic experiments

Photocatalytic studies were carried out using a 450 W Xenon arc lamp (Oriel, Newport, USA) along with a water filter to cut down IR radiation and glass cut off filters, Melles Griot-03FCG057 to permit only visible light (400 nm ≤ λ ≤ 800 nm) and Melles Griot-03SWP602 to permit only UV light (λ ≤ 400 nm) radiations as desired. The experimental details of the photochemical reactor have been reported earlier [17]. A typical experiment of degradation was carried out as follows: 0.2 g of the catalyst was added to 100 ml of aqueous solution of Rh B with an initial concentration of 5×10^{-6} mol/L for visible irradiation experiments. Prior to irradiation, the suspension of the catalyst and dye solutions was stirred in dark for 30–60 min, so as to reach the equilibrium adsorption. 5 ml aliquots were pipetted out periodically from the reaction mixture. The solutions were centrifuged and the concentration of the solutions was determined by measuring the maximum absorbance (λ_{max} = 552 nm).

3. Results and discussion

3.1. Synthetic attempts and products characterization for cation (Sn^{2+}) substitution in $K_2La_2Ti_3O_{10}$

$K_2La_2Ti_3O_{10}$ has a layered perovskite structure consisting of lanthanum titanium perovskite layers interleaved by K^+ ions [31]. $K_2La_2Ti_3O_{10}$ has been known to crystallize in I4/mmm

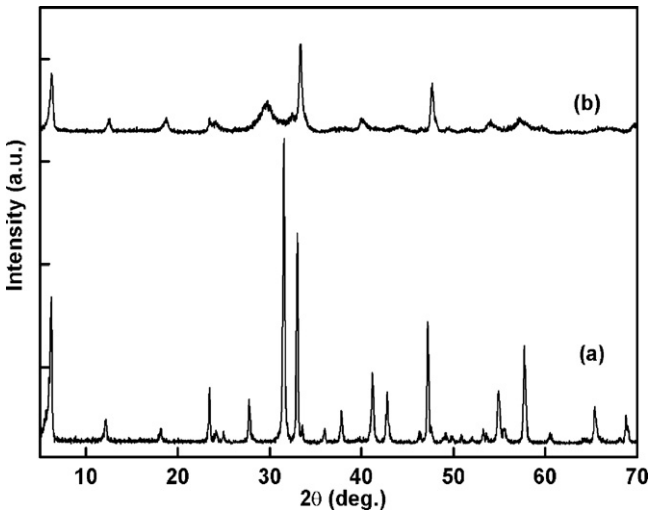

Fig. 1. Powder X-ray patterns of (a) $K_2La_2Ti_3O_{10}$ and (b) Sn^{2+} exchanged $K_2La_2Ti_3O_{10}$.

space group (a = 3.8769(1); c = 29.824(1) Å) and also was found to intercalate water molecules in the interlayer space to form $K_2La_2Ti_3O_{10}{\cdot}2H_2O$ crystallizing in P4/mmm space group (a = 3.8585(1); c = 16.814(1) Å) [31,32]. In the present study, the powder X-ray diffraction of anhydrous $K_2La_2Ti_3O_{10}$ (Fig. 1 and Fig. S1 in the Supporting Information) agreed well with those published earlier [31,32] and the tetragonal lattice parameters were found to be a = 3.848(7) and c = 29.575(1) Å. The aqueous ion-exchange of anhydrous $K_2La_2Ti_3O_{10}$ with $SnCl_2{\cdot}2.0H_2O$ solution at room temperature was sufficient to incorporate Sn^{2+} ions in place of K^+ ions. During the exchange of Sn^{2+} ions, water molecules were also incorporated as in the case of parent $K_2La_2Ti_3O_{10}$. The extent of water intake was estimated to be one water molecule (H_2O) from the loss observed around 100 °C during the thermogravimetric analysis (Fig. S2 in the Supporting Information) of the ion-exchanged product. SEM measurements (Fig. 2) of the parent $K_2La_2Ti_3O_{10}$ and the Sn^{2+} ion-exchanged product revealed that the shape of the crystallites has been retained in the product without any significant variation. Rod and plate like structures of the parent $K_2La_2Ti_3O_{10}$ were preserved during the Sn^{2+} ion-exchange. However, the crystallite agglomerates of the order of 1 μm or less in the Sn^{2+} exchanged $K_2La_2Ti_3O_{10}$ suggested a size reduction (Fig. 2b), possibly because the ion-exchange reaction of $K_2La_2Ti_3O_{10}$ with aqueous $SnCl_2{\cdot}2H_2O$ solution was carried out under ultra sonication, an established procedure to achieve a reduction in the crystallite size [33].

The respective EDAX measurements in Fig. S3 in the Supporting Information yielded 0.45 of Sn and 0.2 of K along with an expected ratio of 2:3 for La:Ti. TGA results (Fig. S2) clearly indicated a loss of 1.0 to 1.5 water molecules up to a temperature of 200 °C and in addition showed a distinctive step corresponding to the loss of one water molecule between temperatures 200 and 400 °C. The initial loss of water after 100 °C substantiates the hydrate formation similar to that of the parent potassium analog. The loss of water at reasonably higher temperatures of 200–400 °C point to the possibility of the presence of protons and Sn^{2+} ions occupying the lattice sites of the vacated potassium ions. This situation is similar to the formation of acid such as $H_2La_2Ti_3O_{10}$ by the treatment of $K_2La_2Ti_3O_{10}$ with a mineral acid [31]. In the present case, the incorporation of protons along with Sn^{2+} ions might balance the charge leading to a product composition of $(Sn_{1.0}K_{0.2}H_{0.9})La_2Ti_3O_{10}{\cdot}1.0H_2O$ based on the EDAX and TGA results.

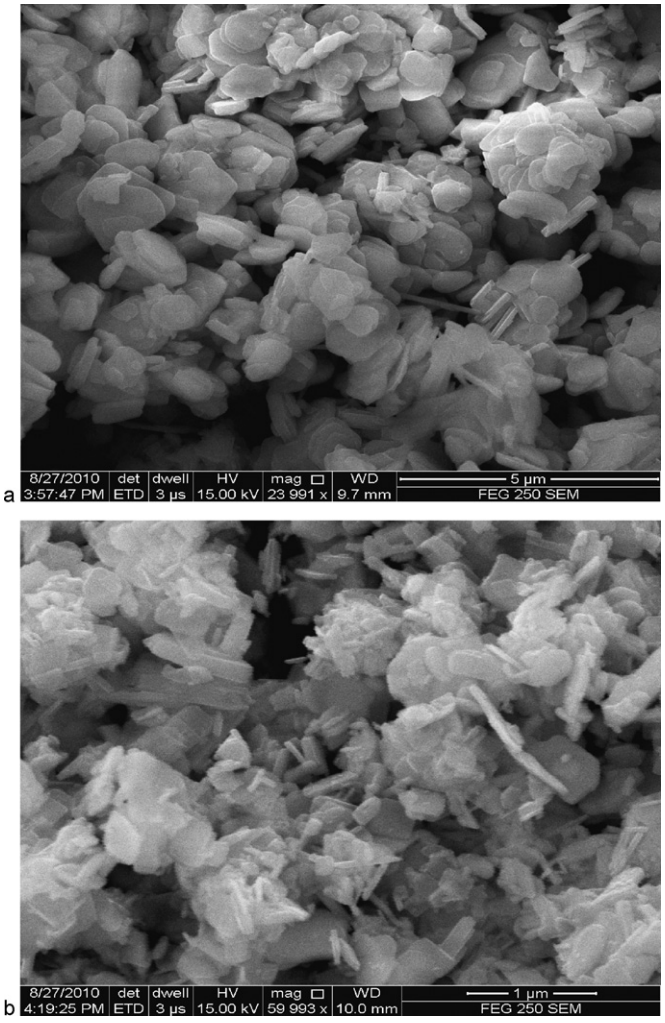

Fig. 2. SEM images of (a) $K_2La_2Ti_3O_{10}$ and (b) Sn^{2+} exchanged $K_2La_2Ti_3O_{10}$.

Considerable changes in the peak shape and intensities have been noticed in the powder X-ray diffraction patterns (Fig. 1). The presence of successive c axis dependent 0 0 l reflections (specifically in the 2θ range of ~5–25°) confirmed the layered structure and a careful analysis of the rest of the reflections indicated the possibility of the occurrence of both the structural types (I4/mmm) or (P4/mmm). Accordingly, Le Bail [34] fit of the powder X-ray diffraction patterns to determine the lattice parameters of Sn^{2+} exchanged product was carried out using TOPAS [35] by considering both the structural types, and we found (Fig. S4) that the majority of the pattern could be indexed based on the I4/mmm structure and the refined lattice parameters are a = 3.808(4); c = 28.87(4) Å). The decrease in the lattice parameters has been found to be consistent with the corresponding decrease (~0.02 Å) in the interplanar distances (d_{hkl}), as compared to the parent anhydrous $K_2La_2Ti_3O_{10}$. The observed changes in the lattice parameters of the Sn^{2+} ion-exchanged product [18] can be attributed to the combined effect of the (i) water of hydration, which would lead to an increase and (ii) to the replacement of smaller Sn^{2+} (ionic radius (VIII), 1.36 Å) ions replacing bigger K^+ (ionic radius (VIII), 1.65 Å) [36–38] ions.

Diffuse reflectance spectra of $K_2La_2Ti_3O_{10}$ and the Sn^{2+} ion-exchanged product are shown (Fig. 3). The absorption band of the Sn^{2+} incorporated product resulted in red shift consistent with its observed yellow color as compared to the white colored parent oxide. The narrowing of the band gap by Sn^{2+} ion-exchange was estimated to be 2.67 eV versus 3.63 eV for the

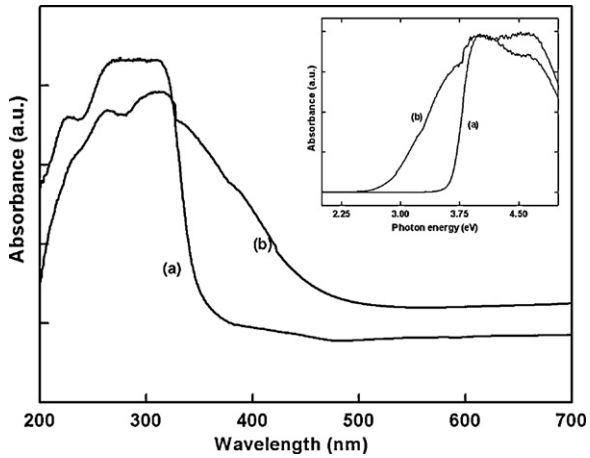

Fig. 3. Diffuse reflectance spectra of (a) $K_2La_2Ti_3O_{10}$ and (b) $(Sn_{1.0}K_{0.2}H_{0.9})La_2Ti_3O_{10}$. Inset shows the corresponding absorbance versus energy in eV.

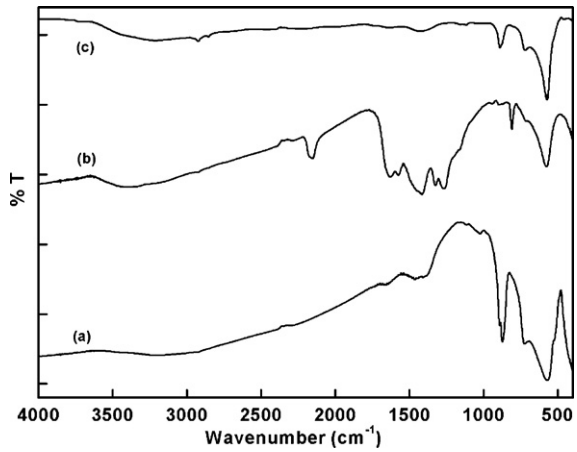

Fig. 5. Infrared spectra of (a) $K_2La_2Ti_3O_{10}$, (b) CN-$K_2La_2Ti_3O_{10}$ and (c) N-$K_2La_2Ti_3O_{10}$.

parent $K_2La_2Ti_3O_{10}$ (inset in Fig. 3). The lowering of the band gap can be related to the valence band formation of Sn 5s and O 2p orbitals and with a conduction band resulting out of Ti 3d orbitals. The band gap reduction due to Sn^{2+} contribution has been well established in many of the mixed metal oxides such as pyrochlore $Sn_{2-x}{}^{2+}(Sn_y{}^{4+}M^{5+}{}_{2-y})O_{7-x-(y/2)}$ (M = Nb, Ta) [39], SnM_2O_6 (M = Nb, Ta) [20], the ion-exchanged layered oxides, $Sn^{2+}/KTiNbO_5$, and $Sn^{2+}/K_4Nb_6O_{17}$ [22], and in the tin antimony pyrochlore oxides ($Sn_{0.92}Sb_2O_6{\cdot}2.0H_2O$, $K_{0.59}Sn_{0.20}SbWO_6{\cdot}1.0H_2O$ and $K_{0.58}Sn_{0.29}TaWO_6{\cdot}1.0H_2O$) [18]. The absorption in the visible region of Sn^{2+} cation exchanged product was possible mostly because of the electronic transition from the valence band of Sn 5s and O 2p orbitals to the conduction band having mainly the valence orbitals (3d) of titanium.

3.2. Synthetic attempts and products characterization for anion substitution (N^{3-}) in $K_2La_2Ti_3O_{10}$

Fig. 4 shows the powder X-ray diffraction patterns of $K_2La_2Ti_3O_{10}$ and its urea reacted (at 400 °C in air) product. The diffraction patterns indicate that the layer structure is maintained along with the peak broadening indicating a decrease in the crystallinity of the product. The likelihood of the peak broadening noticed in the powder X-ray diffraction pattern might also arise due to the presence of structures corresponding to that of the parent

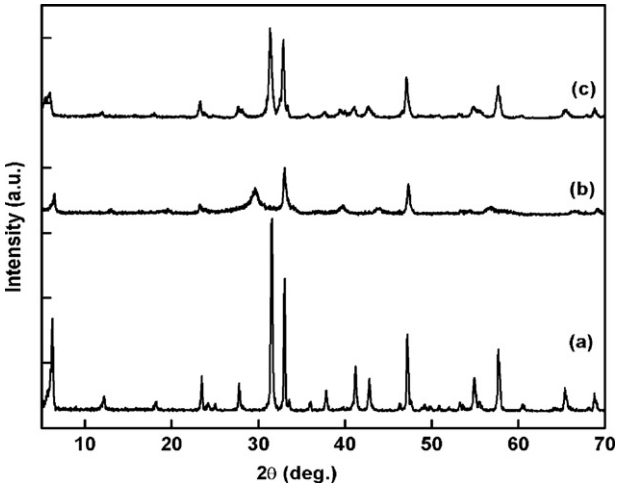

Fig. 4. Powder X-ray patterns of (a) $K_2La_2Ti_3O_{10}$, (b) CN-$K_2La_2Ti_3O_{10}$ and (c) N-$K_2La_2Ti_3O_{10}$.

anhydrous and hydrated forms in the end products. Le Bail fit of the powder X-ray diffraction patterns to determine the lattice parameters of the urea treated product was carried out by considering both the structural types, and we found (Fig. S5 in the Supporting Information) that the majority of the pattern could be indexed based on the P4/mmm structure and the refined lattice parameters are $a = 3.857(1)$; $c = 14.692(5)$ Å). The reduction in the c parameter implies that the polymer might very well be dispersed throughout the solid without specifically occupying the interlayer space.

The TGA of the urea reacted $K_2La_2Ti_3O_{10}$ product when carried out with a heating rate 10 °C/min (Fig. S5 in the Supporting Information) exhibited a very high percentage loss of about 25% between temperatures 450 and 800 °C. The TGA plot showed a small decrease (around 0.05%) up to 150 °C. A small weight increase (around 1.5%) has been noticed before the substantial weight loss (25%) due to the CN polymer. In order to verify the weight increase of 1.5% against the weight loss of 25%, we carried out the same experiment with a heating rate of 3 °C. This TGA output (inset in Fig. S6) resulted only in a continuous loss leading to the decomposition and removal of the CN based polymer. Subsequent analysis of the FTIR spectra showed several strong bands in the range 1200–1700 cm^{-1} (Fig. 5), suggesting the presence of residual carbon products of urea decomposition. IR spectrum of the parent $K_2La_2Ti_3O_{10}$ has also been shown for comparison, wherein the peaks corresponding to the O–Ti–O bonding were only present in the range 500–1000 cm^{-1}. The decomposition products of urea are complicated and the products have been identified as C_3N_4 [24], along with various other carbon and nitrogen (CN) containing heterocyclics. The broad band near 3400 cm^{-1} corresponds to the N–H stretching vibration. The peak noticed around 2150 cm^{-1} can be assigned to the N=C=O stretching or –N=C=N stretching [40]. The strong bands in the range 1200–1700 cm^{-1} are correlated to the skeletal stretching vibrations of the aromatic rings and can be taken as the finger print for the presence of CN polymers. An out of plane bending mode of these heterocyclics has been noticed around 800 cm^{-1} [29,30]. Morphology from SEM measurements of the CN sensitized $K_2La_2Ti_3O_{10}$ (CN-$K_2La_2Ti_3O_{10}$) powder samples (Fig. 6) neither showed any marked change from the morphology of $K_2La_2Ti_3O_{10}$ (Fig. 2), nor the presence of CN polymers. The presence of CN polymers was only detected from the respective TEM images (Fig. 7). The images in addition to plate and rod like features confirmed the presence of polymeric network.

Since the nitridation of urea resulted in CN polymers sensitized $K_2La_2Ti_3O_{10}$, for comparison we attempted an alternate nitridation experiment of heating the parent oxide under NH_3 vapor with N_2 purge gas around 400 °C. The color of the product remained sim-

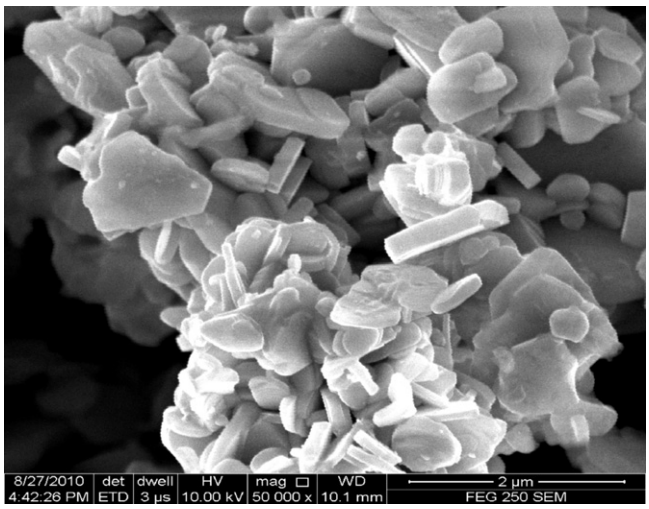

Fig. 6. SEM image of CN-$K_2La_2Ti_3O_{10}$.

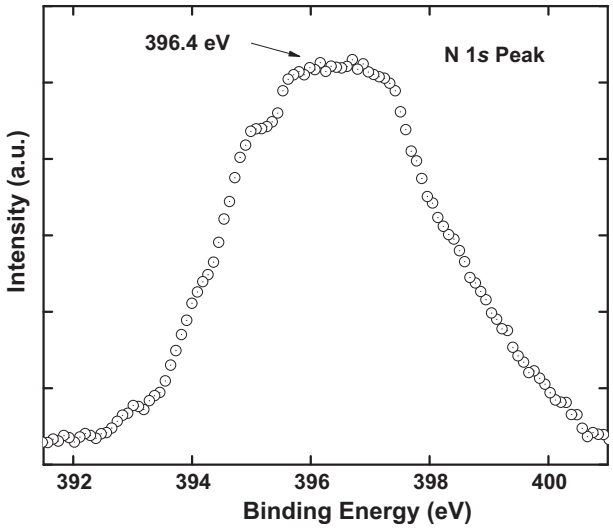

Fig. 8. The XPS spectra of N1 s peak CN-$K_2La_2Ti_3O_{10}$.

ilar and the powder X-ray diffraction pattern (Fig. 4c) indicated a systematic increase of d values (~0.02 Å) with the parent structure intact. The peak broadening has been found to be less than that of the CN sensitized product (Fig. 4b). The corresponding IR spectra (Fig. 5c) also did not show the strong peaks in the range 1200–1700 cm^{-1}, except for the bending vibration mode of N–H bond at 1423 cm^{-1} thereby confirming the doping of nitrogen in $K_2La_2Ti_3O_{10}$. There seems to be a possibility of N–O because of the additional absorption peak around 720 cm^{-1}. Usually, the infrared bands of NO_2 were identified by the strong peak around 1618 cm^{-1} (anti symmetric stretch), weak absorption around 1318 cm^{-1} (symmetric stretch), and the strong peak around 750 cm^{-1} (bending) [41]. However, in the present case, this absorption peak around 720 cm^{-1} has been consistently present in the parent, ammonia treated and urea treated $K_2La_2Ti_3O_{10}$ (Fig. 5) and naturally been assigned to the presence of the parent oxide host and the N–O possibility was therefore excluded. Our results based on FTIR results agreed very well with the only other report of nitrogen doping in $K_2La_2Ti_3O_{10}$, wherein the nitridation was carried out by immersing the parent powder successively in aqueous nitric acid and ammonia solutions, followed by heating in nitrogen gas at 400 °C [42].

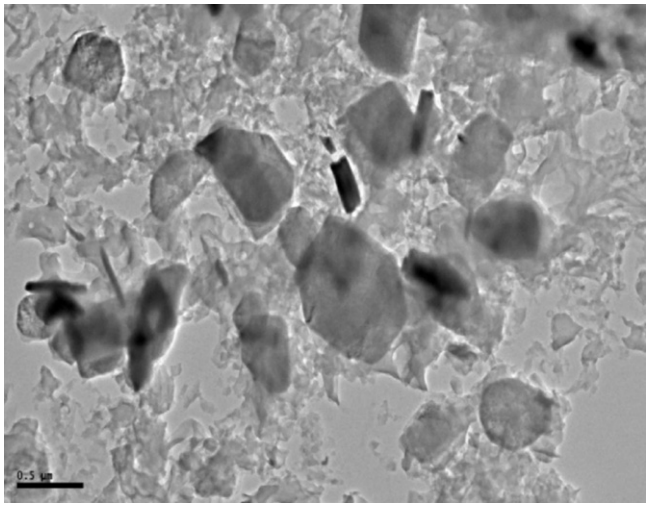

Fig. 7. TEM image of CN-$K_2La_2Ti_3O_{10}$.

Additional information regarding the state of nitrogen in the urea and ammonia treated $K_2La_2Ti_3O_{10}$ has been studied by recording the XPS profiles. Usually, the presence of N^{3-} was confirmed by the observation of N 1s peak with the binding energy around 396 eV [43]. In the present case, the N 1s peak was absent in both the parent $K_2La_2Ti_3O_{10}$ and the ammonia treated $K_2La_2Ti_3O_{10}$. However, we observed a strong N 1s peak around 396.4 eV (Fig. 8), confirming the presence nitrogen in the urea treated $K_2La_2Ti_3O_{10}$. The ammonia treated $K_2La_2Ti_3O_{10}$, however showed a shift in the Ti 2p peak (Fig. S7 in the Supporting Information). In the parent oxide the Ti $2p_{3/2}$ peak was around 458.12 eV, while Ti $2p_{3/2}$ peak was shifted to 457.65 eV in the ammonia treated product. Nitrogen doping in TiO_2 has often resulted in similar shift in their respective Ti $2p_{3/2}$ peak. For example, a lowering of the binding energy up to 0.8 eV has been reported in the Degussa P25 TiO_2 [41]. The binding energy of the Ti $2p_{3/2}$ for the parent (TiO_2 without any nitrogen) and the nitridated TiO_2, have been found to be 459.5 eV and 458.7 eV [41]. The XPS results also led to the conclusion of higher amount of nitrogen in the urea treated sample as indicated by the N 1s peak along with a negligible amount of nitrogen as indicated by the shift in the binding energy of the titanium based ($Ti2p_{3/2}$) peak in the ammonia treated $K_2La_2Ti_3O_{10}$.

Optical absorption property by the UV–visible diffuse reflectance spectra of the CN polymer sensitized (CN-$K_2La_2Ti_3O_{10}$) and nitrogen doped (N-$K_2La_2Ti_3O_{10}$) oxides resulted in red shifts relative to $K_2La_2Ti_3O_{10}$ (Fig. 9). Nitrogen doping has been known to shift of the absorption edge towards higher wavelengths because of the contribution of nitrogen 2p orbitals to the valence band comprised of oxygen 2p orbitals, thereby moving the valence band upwards. Simple doping of nitrogen in place of oxygen in N-$K_2La_2Ti_3O_{10}$ has resulted in a band gap reduction from 3.63 eV ($K_2La_2Ti_3O_{10}$) to 3.59 eV (N-$K_2La_2Ti_3O_{10}$), which is comparable with the earlier observed band gap reduction of 3.69 eV ($K_2La_2Ti_3O_{10}$) to 3.44 eV ($K_2La_2Ti_3O_{10-x}N_x$) [42]. If additionally, CN polymers get incorporated as in the present case of CN-$K_2La_2Ti_3O_{10}$, the UV–visible absorption spectra (Fig. 9) showed in a larger red shift of about 100 nm. The band gap was reduced to 2.92 eV for the CN polymers incorporated nitrogen doped $K_2La_2Ti_3O_{10}$. C_3N_4 itself has been known to absorb visible light with a band gap of 2.7 eV, and the noticeable reduction in the band gap (0.71 eV) of CN-$K_2La_2Ti_3O_{10}$ (inset in Fig. 9) could only be explained by the presence of CN polymers, rather than by simple doping of nitrogen for oxygen.

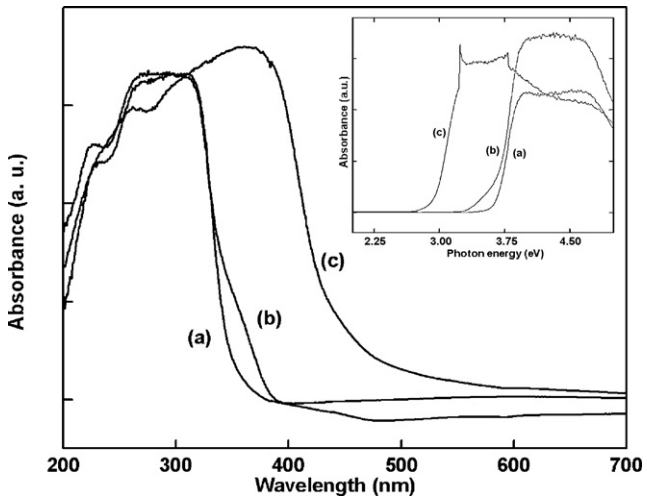

Fig. 9. Diffuse reflectance spectra of (a) $K_2La_2Ti_3O_{10}$, (b) N-$K_2La_2Ti_3O_{10}$ and (c) CN-$K_2La_2Ti_3O_{10}$. Inset shows the corresponding absorbance versus energy in eV.

3.3. Influence on the visible photocatalytic activities by cation (Sn^{2+}) and CN polymers with anion (N^{3-}) incorporation in $K_2La_2Ti_3O_{10}$

Decomposition of Rh B solution was investigated under visible light (400 nm ≤ λ ≤ 800 nm). Fig. 10 shows the rates of decomposition of Rh B for $K_2La_2Ti_3O_{10}$ and Sn^{2+} exchanged $K_2La_2Ti_3O_{10}$, along with the photolysis of Rh B under visible light without any catalyst. For comparison, we have also included the rate of decomposition of Rh B by the well known Degussa P25 TiO_2. It is evident that the photodecomposition of Rh B is negligible in the absence of any catalyst and also in the presence of the parent $K_2La_2Ti_3O_{10}$. The parent oxide did not show any visible absorption and has been found to decompose Rh B only under UV light. TiO_2 although not expected to know any visible activity based on its band gap (E_g = 3.2 eV), was found to decompose Rh B under visible irradiation. This particular degradation of Rh B under visible light has been clarified and been attributed to the sensitization process in which the excited dye molecule efficiently transfers the electron to the conduction band of the specific catalyst semiconductor and initiates the photodegradation process [44]. Almost a similar rate of degradation has been found

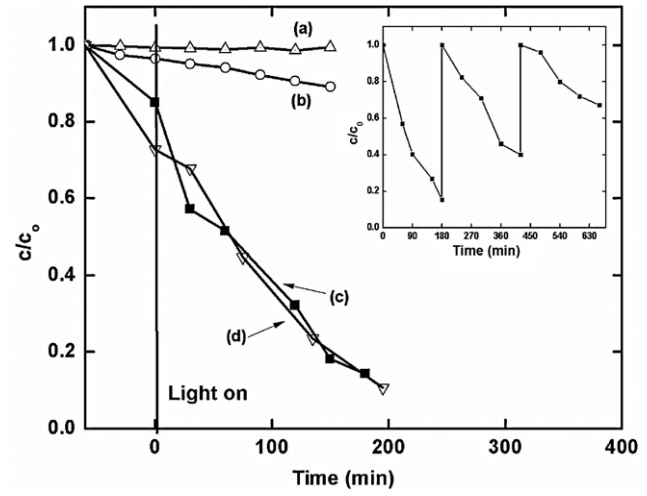

Fig. 10. Photodegradation of Rh B solution with time under visible radiation: (a) Rh B blank, (b) Rh B on $K_2La_2Ti_3O_{10}$, (c) Rh B on Degussa P25 TiO_2 (0.05 g of surface area 55 m^2/g) and (d) Rh B on $(Sn_{1.0}K_{0.2}H_{0.9})La_2Ti_3O_{10}$. Inset shows repeated runs of photodegradation of Rh B solution by $(Sn_{1.0}K_{0.2}H_{0.9})La_2Ti_3O_{10}$.

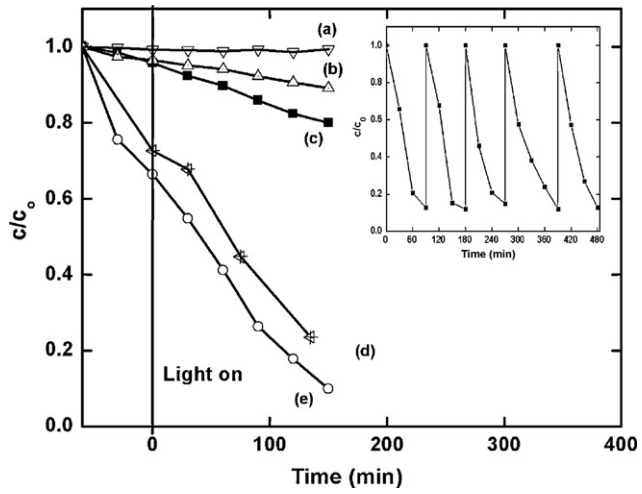

Fig. 11. Photodegradation of Rh B solution with time under visible radiation: (a) Rh B blank, (b) Rh B on $K_2La_2Ti_3O_{10}$, (c) Rh B on N-$K_2La_2Ti_3O_{10}$, (d) Rh B on Degussa P25 TiO_2 (0.05 g of surface area 55 m^2/g) and (e) Rh B on CN-$K_2La_2Ti_3O_{10}$. Inset shows repeated runs of degradation of Rh B. solution by CN-$K_2La_2Ti_3O_{10}$.

for the Sn^{2+}-exchanged sample, $(Sn_{1.0}K_{0.2}H_{0.9})La_2Ti_3O_{10}\cdot 1.0H_2O$ under visible light irradiation (Fig. 10). The photocatalyst has been found to be useful for the additional cycles of decomposition of Rh B, with a moderate decrease in the rate of decomposition (inset in Fig. 10).

CN-$K_2La_2Ti_3O_{10}$ showed higher decomposition rate for Rh B dye as compared to nitrogen doped N-$K_2La_2Ti_3O_{10}$ (Fig. 11). The aqueous Rh B solution has the maximum absorbance around 552 nm and the solution turned colorless within 150 min using 0.2 g of the catalyst CN-$K_2La_2Ti_3O_{10}$. The rate of decomposition was found to be slightly higher than that observed for P25 TiO_2 under similar experimental conditions. The inset in Fig. 11 shows that the CN polymer sensitized $K_2La_2Ti_3O_{10}$ sample was active for the successive cycles of decomposition with similar rates of decomposition of Rh B under visible light irradiation.

Lowering of the energy gaps was achieved successfully for the layered perovskite $K_2La_2Ti_3O_{10}$ as a result of incorporation of Sn^{2+} and by nitrogen doping coupled with CN polymer sensitization. Both cationic and anionic substitutional attempts resulted in corresponding red shift in absorption edges as compared to the parent $K_2La_2Ti_3O_{10}$. The lowering of the band gap was as expected by the contribution of Sn 5s orbitals to the O2p orbitals in the formation of the valence band. Nitridation using urea resulted in nitrogen doping with the additional sensitization by the presence of carbon nitride (CN) polymers, which again was responsible for visible light absorption. The product oxides obtained as a result of cation and anion targeted substitutional studies have been found to be useful for the visible light photocatalytic decomposition of organic dyes such as rhodamine B.

Acknowledgments

The authors thank the University of Delhi for the financial support under the "Scheme to strengthen R&D Doctoral Research Program" and the Nano Mission project under the Department of Science and Technology, Government of India. We thank Dr. R. Nagarajan, Department of Chemistry, University of Delhi for extending some of the experimental facilities and for constant support. Thanks are also to M. Tech, Nanoscience, University of Delhi for Powder X-ray diffraction facility. V.K. thanks the Department of Science and Technology, Government of India for the project assistantship.

Appendix A. Supplementary data

Supplementary data associated with this article can be found, in the online version, at doi:10.1016/j.jhazmat.2011.02.064.

References

[1] H.W. Eng, P.W. Barnes, B.M. Auer, P.J. Woodward, Investigations of the electronic structure of d^0 transition metal oxides belonging to the perovskite family, Solid State Chem. 175 (2003) 94–109.
[2] A. Fujishima, K. Honda, Electrochemical photolysis of water at a semiconductor electrode, Nature (London) 238 (1972) 37–38.
[3] M.R. Hoffman, S.T. Martin, W. Choi, D.W. Bahnemann, Environmental applications of semiconductor photocatalysis, Chem. Rev. 95 (1995) 69–96.
[4] O. Carp, C.L. Huisman, A. Reller, Photoinduced reactivity of titanium dioxide, Prog. Solid State Chem. 32 (2004) 33–177.
[5] A. Mills, S.L. Hunte, An overview of semiconductor photocatalysis, J. Photochem. Photobiol. A: Chem. 108 (1997) 1–35.
[6] H. Zhang, G. Chen, D.W. Bahnemann, Photoelectrocatalytic materials for environmental applications, J. Mater. Chem. 19 (2009) 5089.
[7] R. Asahi, T. Morikawa, T. Ohwaki, K. Aoki, Y. Taga, Visible-light photocatalysis in nitrogen-doped titanium oxides, Science 293 (2001) 269–271.
[8] S. Sakthivel, H. Kisch, Photocatalytic and photoelectrochemical properties of nitrogen-doped titanium dioxide, Chem. Phys. Chem. 4 (2003) 487–490.
[9] X. Chen, C.J. Burda, The electronic origin of the visible-light absorption properties of C-, N- and S-doped TiO_2 nanomaterials, J. Am. Chem. Soc. 130 (2008) 5018.
[10] L. Zhao, X. Chen, Y. Wang, W. Wei, Y. Sun, M. Antonietti, M.M. Titirici, One-step solvothermal synthesis of a carbon@TiO_2 dyade structure effectively promoting visible-light photocatalysis, Adv. Mater. 22 (2010) 3317–3321.
[11] H. Kisch, S. Sakthivel, M. Janczarek, D. Mitoraj, A low-band gap, nitrogen-modified titania visible-light photocatalyst, J. Phys. Chem. C 111 (2007) 11445–11449.
[12] Y. Cong, J. Zhang, F. Chen, M. Anpo, Synthesis and characterization of nitrogen-doped TiO_2 nanophotocatalyst with high visible light activity, J. Phys. Chem. C 111 (2007) 6976–6982.
[13] J. Fang, F. Wang, K. Qian, H. Bao, Z. Jiang, W. Huang, Bifunctional N-doped mesoporous TiO_2 photocatalysts, J. Phys. Chem. C 112 (2008) 18150–18156.
[14] F.E. Osterloh, Inorganic materials as catalysts for photochemical splitting of water, Chem. Mater. 20 (2008) 35–54.
[15] T. Takata, Y. Furumi, K. Shinohara, A. Tanaka, M. Hara, J.N. Kondo, K. Domen, Photocatalytic decomposition of water on spontaneously hydrated layered perovskites, Chem. Mater. 9 (1997) 1063.
[16] R.E. Schaak, T.E. Mallouk, Perovskites by design: a toolbox of solid-state reactions, Chem. Mater. 14 (2002) 1455–1471.
[17] J. Singh, S. Uma, Efficient photocatalytic degradation of organic compounds by ilmenite $AgSbO_3$ under visible and UV light irradiation, J. Phys. Chem. C 113 (2009) 12483–12488.
[18] S. Uma, J. Singh, V. Thakral, Facile room temperature ion-exchange synthesis of Sn^{2+} incorporated pyrochlore-type oxides and their photocatalytic activities, Inorg. Chem. 48 (2009) 11624.
[19] V. Thakral, S. Uma, Investigation of visible light photocatalytic behavior of $Bi_4V_2O_{11-\delta}$ and BIMEVOX (ME = Al, Ga) oxides, Mater. Res. Bull. 45 (2010) 1250.
[20] Y. Hosogi, Y. Shimodaira, H. Kato, H. Kobayashi, A. Kudo, Role of Sn^{2+} in the band structure of SnM_2O_6 and $Sn_2M_2O_7$ (M = Nb and Ta) and their photocatalytic properties, Chem. Mater. 20 (2008) 1299–1307.
[21] I.S. Cho, C.H. Kwak, D.W. Kim, S. Lee, K.S. Hong, Photophysical, photoelectrochemical and photocatalytic properties of novel $SnWO_4$ oxide semiconductors with narrow band gaps, J. Phys. Chem. C 113 (2009) 10647–10653.
[22] Y. Hosogi, H. Kato, A. Kudo, Photocatalytic activities of layered titanates and niobates ion-exchanged with Sn^{2+} under visible light irradiation, J. Phys. Chem. C 112 (2008) 17678–17682.
[23] X. Li, N. Kikugawa, J. Ye, Nitrogen-doped lamellar niobic acid with visible light-responsive photocatalytic activity, Adv. Mater. 20 (2008) 3816–3819.
[24] G. Liu, L. Wang, C. Sun, X. Yan, X. Wang, Z. Chen, S.C. Smith, H.M. Cheng, G.Q. Lu, Band-to-band visible-light photon excitation and photoactivity induced by homogeneous nitrogen doping in layered titanates, Chem. Mater. 21 (2009) 1266–1274.
[25] W. Wei, Y. Dai, M. Guo, L. Yu, B. Huang, Density functional characterization of the electronic structure and optical properties of N-doped, La-doped, and N/La-codoped $SrTiO_3$, J. Phys. Chem. C 113 (2009) 15046–15050.
[26] X. Wang, K. Maeda, A. Thomas, K. Takanabe, G. Xin, J.M. Carlsson, K. Domen, M. Antonietti, A metal-free polymeric photocatalyst for hydrogen production from water under visible light, Nat. Mater. 8 (2009) 76–80.
[27] X. Wang, X. Chen, A. Thomas, X. Fu, M. Antonietti, Metal-containing carbon nitride compounds: a new functional organic–metal hybrid material, Adv. Mater. 21 (2009) 1609–1612.
[28] D. Mitoraj, H. Kisch, The nature of nitrogen-modified titanium dioxide photocatalysts active in visible light, Angew. Chem. Int. Ed. 47 (2008) 9975–9978.
[29] L. Guoqiang, N. Yang, W. Wang, W.F. Zhang, Synthesis, photophysical and photocatalytic properties of N-doped sodium niobate sensitized by carbon nitride, J. Phys. Chem. C 113 (2009) 14829–14833.
[30] Q. Li, B. Yue, H. Iwai, T. Kako, J. Ye, Carbon nitride polymers sensitized with N-doped tantalic acid for visible light-induced photocatalytic hydrogen evolution, J. Phys. Chem. C 114 (2010) 4100–4105.
[31] J. Gopalakrishnan, V. Bhat, $A_2La_2Ti_3O_{10}$ (A = potassium or rubidium; Ln = lanthanum or rare earth): a new series of layered perovskites exhibiting ion exchange, Inorg. Chem. 26 (1987) 4299–4301.
[32] K. Toda, J. Watanabe, M. Sat, Crystal structure determination of ion-exchangeable layered perovskite compounds, $K_2La_2Ti_3O_{10}$ and $Li_2La_2Ti_3O_{10}$, Mater. Res. Bull. 31 (1996) 1427–1435.
[33] K.S. Suslick, Sonochemistry, Science 247 (1990) 1439–1445;
A. Gedanken, Using sonochemistry for the fabrication of nanomaterials, Ultrason. Sonochem. 11 (2004) 47–55;
T.J. Mason, Use of ultrasound in chemical synthesis, Ultrasonics 24 (1986) 245–253.
[34] A. Le Bail, H. Duroy, J.L. Fourquet, Ab-initio structure determination of $LiSbWO_6$ by X-ray powder diffraction, Mater. Res. Bull. 23 (1988) 447–452.
[35] A.A. Coelho, TOPAS Version 3.1, Bruker AXS GmbH, Karlsruhe, Germany, 2003.
[36] O. Muller, R. Roy, The Major Ternary Structural Families, Springer-Verlag, New York, 1974.
[37] R.D. Shannon, C.T. Prewitt, Effective ionic radii in oxides and fluorides, Acta Crystallogr. B25 (1969) 925.
[38] R.D. Shannon, C.T. Prewitt, Revised values of effective ionic radii, Acta Crystallogr. B26 (1970) 1046.
[39] H. Mizoguchi, A. Wattiaux, R. Kykneshi, J. Tate, A.W. Sleight, M.A. Subramanian, Synthesis and characterization of Sn^{2+} oxides with the pyrochlore structure, Mater. Res. Bull. 43 (2008) 1943.
[40] D.J.V. Pulsipher, I.T. Martin, E.R. Fisher, Controlled nitrogen doping and film colorimetrics in porous TiO_2 materials using plasma processing, ACS Appl. Mater. Interfaces 2 (2010) 1743–1753.
[41] X. Chen, Y. Lou, A.C.S. Samia, C. Burda, J.L. Gole, Formation of oxynitride as the photocatalytic enhancing site in nitrogen-doped titania nanocatalysts: comparison to a commercial nanopowder, Adv. Funct. Mater. 15 (2005) 41–49.
[42] Y. Huang, Y. Wei, S. Cheng, L. Fan, Y. Li, J. Lin, J. Wu, Photocatalytic property of nitrogen-doped layered perovskite $K_2La_2Ti_3O_{10}$, Sol. Energy Mater. Sol. Cells 94 (2010) 761–766.
[43] N.C. Saha, H.G. Tompkins, Titanium nitride oxidation chemistry: an X-ray photoelectron spectroscopy study, J. Appl. Phys. 72 (1992) 3072–3080.
[44] F. Zhang, J. Zhao, L. Zang, T. Shen, H. Hidaka, E. Pelizzetti, N. Serpone, Photoassisted degradation of the dye pollutants in aqueous TiO_2 dispersions under irradiation by visible light, J. Mol. Catal. A: Chem. 120 (1997) 173–178.